Int. J. Cancer: **122,** 1145–1154 (2008)

Synthesis and biological evaluation of an albumin-binding prodrug of doxorubicin that is cleaved by prostate-specific antigen (PSA) in a PSA-positive orthotopic prostate carcinoma model (LNCaP)

Ralph Graeser[1], Da-Eun Chung[2], Norbert Esser[1], Sandra Moor[1], Christoph Schächtele[1], Clemens Unger[2] and Felix Kratz[2]*

[1]*ProQinase GmbH, Freiburg, Germany*
[2]*Department of Medical Oncology, Clinical Research, Tumor Biology Center, Freiburg, Germany*

The prostate-specific antigen (PSA) is a serine protease that is over-expressed in prostate carcinoma and represents a molecular target for selectively releasing an anticancer agent from a prodrug formulation. We have recently investigated a macromolecular prodrug strategy for improved cancer chemotherapy based on 2 features: (*i*) rapid and selective binding of thiol-reactive prodrugs to the cysteine-34 position of endogenous albumin after intravenous administration, and (*ii*) enzymatic release of the albumin-bound drug at the tumor site (Mansour *et al.*, Cancer Res 2003, 63, 4062–4066). In this work, we describe an albumin-binding prodrug, EMC-Arg-Ser-Ser-Tyr-Tyr—Ser-Arg-DOXO [EMC: ε-Maleimidocaproic acid; DOXO = doxorubicin; X = amino acid] that is cleaved by PSA. Because of the incorporation of 2 arginine residues, the prodrug exhibited excellent water-solubility and was rapidly and selectively bound to endogenous albumin. Incubation studies with PSA and tumor homogenates from PSA-positive tumors (LNCaP) demonstrated that the albumin-bound form of the prodrug was efficiently cleaved by PSA at the P_1–P_1' scissile bond releasing the doxorubicin dipeptide H-Ser-Arg-DOXO, which was further degraded to doxorubicin as the final cleavage product. In cell culture experiments, the prodrug was ~100-fold less active against LNCaP cells than the free drug. In contrast, in a mouse model of human prostate cancer using luciferase transduced LNCaP cells orthotopically implanted in SCID mice, the prodrug showed enhanced antitumor efficacy when compared to doxorubicin. Doxorubicin treatment at a dose of 2 × 4 mg/kg caused significant weight loss and mortality (−25%), and did not result in a significant antitumor response at the end of the experiment. The prodrug at 3 × 12 mg/kg doxorubicin equivalents, however, was well tolerated and induced a significant reduction in tumor size of 62% (±25%, **$p = 0.003$) as well as a decrease of the metastatic burden in the lungs as detected in luciferase assays (−50%, SD ± 115%, *$p = 0.038$).

Key words: doxorubicin; macromolecular prodrug; human serum albumin; PSA; orthotopic animal model; LNCaP; luciferase; *in vivo* bioluminescence

Hormone refractory prostate cancer responds unfavorably to chemotherapy. The best results to date are achieved with Taxotere.[1] To improve prostate cancer therapy, tumor-specific delivery of anticancer agents to the primary tumor and metastases is a goal worth pursuing.

For selectively releasing anticancer agents, the prostate-specific antigen (PSA) is especially attractive as a target protease because it is solely expressed in prostate tissue and prostate carcinoma in prostate cancer patients with high levels up to mg/g present in human prostate carcinoma.[2,3] PSA is a serine protease that belongs to the kallikrein gene family with chymotrypsin-like activity that is involved in the hydrolytic processing of semenogelins (cleavage of the semenal fluid proteins semenogelin I and II), which is required for liquefaction of seminal fluids.[2,3] Over-expression of PSA has primarily been demonstrated in prostate carcinoma and at low levels in breast cancer.[4–8]

We have recently developed an albumin-binding prodrug of doxorubicin that is cleaved by PSA, *i.e.*, EMC-Arg-Arg-Ser-Ser-Tyr-Tyr—Ser-Gly-DOXO (EMC = 6-maleimidocaproic acid; DOXO = doxorubicin.[9] Our drug targeting strategy is based on 2 features[10–12]: (*i*) *in situ* binding of a thiol-binding prodrug to the cysteine-34 position of circulating albumin after intravenous administration with subsequent accumulation of the drug albumin conjugate in the tumor because of passive targeting; (*ii*) release of the albumin-bound drug at the tumor site because of the incorporation of a cleavable bond between the drug and the carrier.

EMC-Arg-Arg-Ser-Ser-Tyr-Tyr—Ser-Gly-DOXO is cleaved efficiently by PSA between Tyr and Ser releasing the doxorubicin dipeptide H-Ser-Gly-DOXO. Two arginine residues were introduced into the peptide linker to render the prodrug water-soluble. The prodrug showed no *in vivo* activity in the PSA-negative PC-3 model, but good activity in the CWR22 PSA-positive model that was comparable to doxorubicin.[9] Incubation studies with CWR22 tumor homogenates revealed, however, that the full potential of EMC-Arg-Arg-Ser-Ser-Tyr-Tyr—Ser-Gly-DOXO had not been exploited considering that a less active doxorubicin dipeptide DOXO-Gly-Ser and not doxorubicin was released in PSA-positive prostate carcinoma tissues.

The goal of the present work was to optimize the structure of this prodrug that would allow doxorubicin to be released in prostate tumors as the final cleavage product. In recent work, we discovered that among a spectrum of doxorubicin amino acid derivatives *N*-(L-arginine)doxorubicin (H-Arg-DOXO) was the only compound that was efficiently cleaved to doxorubicin in tumor homogenates at pH 7.4.[13] We reasoned that replacing Gly by Arg at the C-terminal position could behave in a similar way and also release doxorubicin through the action of other proteases in tumor homogenates. Consequently, we developed the doxorubicin prodrug EMC-Arg-Ser-Ser-Tyr-Tyr—Ser-Arg-DOXO (**PSA5**) that is shown in Figure 1.

To test novel antitumor agents in a setting that reflects the human disease better than subcutaneous models, we have developed orthotopic models for pancreas and kidney cancer using luciferase marked tumor cells. Bioluminescence mediated detection and observation of the tumors over the period of a treatment allows the randomization of tumor bearing animals, exclusion of animals without or with aberrantly growing tumors as well as the monitoring of drug effects on the tumor. For our study, the PSA-positive LNCaP prostate tumor cell line, transduced with a construct expressing a Luciferase–Neomycin resistance fusion protein, was implanted orthotopically into the prostates of SCID mice. When implanted orthotopically, this cell line metastasizes to local lymph nodes, lungs and other organs[14–17] thus drug effects on metastases can be investigated as well.

In this work we describe the synthesis of the novel prodrug, its cleavage profile and *in vitro* and *in vivo* activity in comparison to free doxorubicin.

***Correspondence to:** Department of Medical Oncology, Clinical Research, Tumor Biology Center, Breisacher Straße 117, D-79106 Freiburg, Federal Republic of Germany. Fax: +0049-761-2062905.
E-mail: felix@tumorbio.uni-freiburg.de
Received 14 May 2007; Accepted after revision 25 June 2007
DOI 10.1002/ijc.23050
Published online 31 October 2007 in Wiley InterScience (www.interscience.wiley.com).

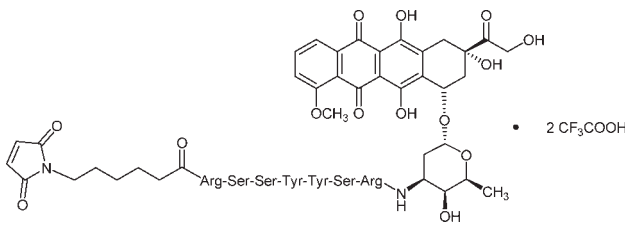

FIGURE 1 – Structure of the albumin-binding prodrug **PSA5** containing a PSA-specific substrate.

Results

Chemistry

The albumin-binding prodrug **PSA5** (see Fig. 1) was synthesized from doxorubicin, using a Fmoc-based strategy. H-Arg-DOXO was obtained by reacting doxorubicin with Fmoc-Arg-OH in anhydrous *N*,*N*-dimethylformamide (DMF) in the presence of *N*-ethyldiisopropylamine (DIEA) and *O*-(azabenzotriazol-1-yl)-*N*,*N*,*N*′,*N*′-tetramethyluronium hexafluorophosphate (HATU) as the coupling agent, removing the Fmoc-group with piperidine and isolating the product with diol column chromatography. In a next step, a serine residue was introduced by reacting H-Arg-DOXO with commercially available Fmoc-Ser-OH in anhydrous DMF in the presence of DIEA and HATU. The protecting group was removed with piperidine and H-Ser-Arg-DOXO was isolated through chromatography on a diol column.

In a final step, EMC-Arg-Ser-Ser-Tyr-Tyr-OH was coupled to H-Ser-Arg-DOXO in anhydrous DMF in the presence of *N*,*N*′-diisopropylcarbodiimide, 1-hydroxybenzotriazole hydrate and 4-methylmorpholine in a one step procedure. **1** was purified through size-exclusion chromatography on Sephadex^{TM} LH-20 followed by reverse phase chromatography (C18 column). The lyophilized red product was characterized by mass spectrometry and purity determined by HPLC. **PSA5** showed excellent water-solubility with up to 10 mg/mL in buffer solutions in the pH-range of 6.0–7.0.

Binding of PSA5 to endogenous albumin in human plasma

To determine the coupling rate and selectivity of **PSA5** for endogenous albumin, the prodrug was incubated with human blood plasma at 37°C, and the samples were subsequently analyzed by reverse phase chromatography. Chromatograms after an incubation time of 5 min, 4, and 24 hr are shown in Figure 2. Protein components were detected at 254 nm and the anthracycline moiety simultaneously at 495 nm. Figure 2 demonstrates rapid and selective binding of **PSA5** to endogenous albumin after 5 min with a distinct single peak at the retention time of ~32 min and with only traces of **PSA5** eluting after ~11 min.

The stability of the albumin conjugate of **PSA5** in human blood plasma was assessed after **PSA5** had been incubated at 37°C with plasma for 5 min, 4, and 24 hr. HPLC chromatograms in Figure 2 shows that the albumin-bound form is relatively stable over 24 hr with ~18% degradation after 24 hr.

To demonstrate that the cysteine-34 position of albumin plays an important role in the coupling step, analogous HPLC experiments were carried out, in which human plasma was preincubated with an excess of EMC (ε-maleimidocaproic acid) prior to incubation with **PSA5** (see Fig. 2). In this experiment, a low degree binding to HSA was observed after incubating plasma with **PSA5**.

Cleavage of the albumin-conjugate of PSA5 by PSA and in LNCaP tumor homogenates

To investigate whether and how fast the albumin conjugate of **PSA5** is cleaved by PSA, the conjugate was incubated with enzymatically active PSA and chromatograms recorded at 495 nm using reverse phase HPLC. Fast and distinct cleavage to H-Ser-Arg-DOXO eluting at 5.4 min was observed after incubating the albumin-conjugate of **PSA5** with PSA after 2 hr (see Fig. 3). After 4 hr of incubation, cleavage to H-Ser-Arg-DOXO was essentially complete.

To assess, whether H-Ser-Arg-DOXO is further degraded in prostate tumors, we incubated this doxorubicin dipeptide with homogenates from LNCaP tumors (PSA levels ~5.6 μg/g). Chromatograms after 0, 2 and 5 hr are shown in Figure 4 demonstrating that H-Arg-DOXO and doxorubicin are formed in a time-dependent manner.

When the albumin conjugate of **PSA5** was incubated with homogenates from LNCaP tumors, cleavage to H-Arg-DOXO and doxorubicin was detected (see Fig. 5).

In vitro *activity of doxorubicin and the albumin-conjugate of PSA5 against the PSA-positive prostate cancer cell line LNCaP LN*

LNCaP LN is the PSA-expressing prostate cancer cell line LNCaP with a stably integrated Luciferase–Neomycin (LN) resistance fusion gene cassette. Cells expressing this fusion protein can be selected by G418, and if injected in mice, be detected *in vivo* through bioluminescence imaging. Because of the activation of **PSA5** by PSA cleavage, the level of PSA expression by the LNCaP LN cells was measured over a period of 96 hr. It was correlated with the number of cells and the expression of luciferase.

When ~200,000 cells were plated in a 6-well plate, the cells grew exponentially for 72 hr; at this time-point the proliferation rate ceased because of cell density (Fig. 6*a*, light and dark grey bars). PSA accumulated over the whole 96-hr period, whereas the expression of luciferase decreased with the slow-down of proliferation (Fig. 6*a*, red and blue bars). PSA levels secreted in the PSA-positive LNCaP cell culture medium was measured using microparticle immunoassay (100.000 cells/mL: ~21 ng/mL after 24 hr, ~75 ng/mL after 48 hr, 150 ng/mL after 72 hr and ~260 ng/mL after 96 hr).

Next, the sensitivity of the LNCaP LN cell line to free doxorubicin as well as the prodrug was tested in proliferation assays. After an incubation of the cells in the presence of either drug for 72 hr, alamar blue was added to the cells to measure mitochondrial activity. After 3 hr, cells were harvested, and the alamar blue conversion was measured. Subsequently, cells were lysed and the luciferase activity of the lysate determined.

Doxorubicin very efficiently killed the LNCaP cells *in vitro* with IC_{50} values of 70 and 140 nM, respectively. The prodrug, on the other hand was ~100-fold less active with IC_{50}values of 8 and 32 μM (Fig. 6*b*).

Antitumor activity of PSA5 and doxorubicin in an ortotopic prostate tumor model (LNCaP)—In vivo *results*

The *in vivo* efficacy of the prodrug was compared to free doxorubicin in a mouse prostate cancer model using LNCaP LN cells orthotopically implanted into the prostates of SCID mice. This technique allows the tumor cells to grow in an environment related to their origin and thus mimics tumor–stromal cell interactions better than subcutaneous models. Furthermore, since lung metastases are reproducibly observed, antimetastatic activity of test compounds can be evaluated. Bioluminescence measurements using the stably integrated luciferase gene were used to monitor the growth of the otherwise undetectable tumors.

Tumor cells were detected as early as 2 days after implantation (Fig. 7*c*). However, since this original activity usually decreases during the establishment of the tumor, bioluminescence signals from day 10 were used to randomize the animals into treatment groups (Fig. 7*a*). The take rate was around 65%, and mice without detectable tumors were excluded from the study.

Based on preliminary toxicity studies, 12 mg/kg doxorubicin equivalents for the prodrug were compared to 4 mg/kg of the free drug. Animals were injected with the drugs once weekly for a pe-

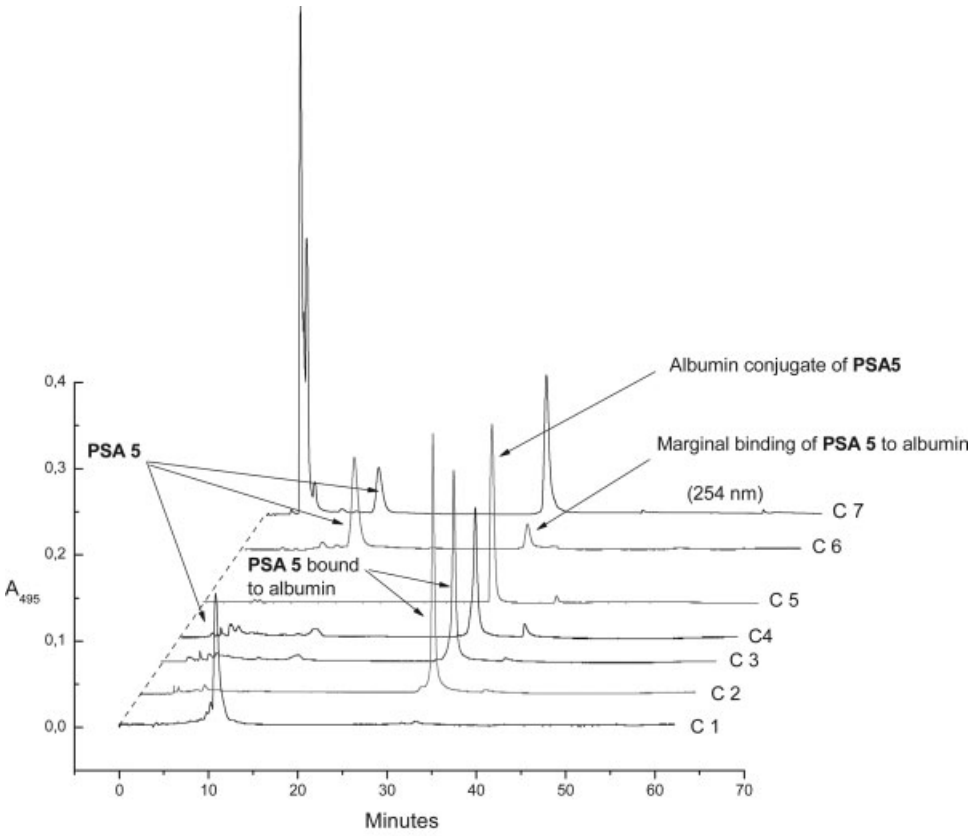

C 1	**PSA5** in glucose-phosphate buffer pH 6.4
C 2	**PSA5** + human blood plasma after 5 min
C 3	**PSA5** + human blood plasma after 4 h
C 4	**PSA5** + human blood plasma after 24 h
C5	Albumin conjugate of **PSA5**
C 6/C 7	**PSA5** + human blood plasma blocked with EMC after 10 min, **C 6:** λ = 254 nm

Figure 2 – Chromatograms of incubation studies of human plasma after 5 min, 4 and 24 hr with **PSA5** at 37°C and chromatograms of incubation studies of human plasma preincubated with an excess of 6-maleimidocaproic acid (EMC) for 2 hr and subsequent incubation with **PSA5** after 15 min at 37°C. Concentration of the anthracycline was 250 μM. Chromatographic conditions: see "Experimental" Section.

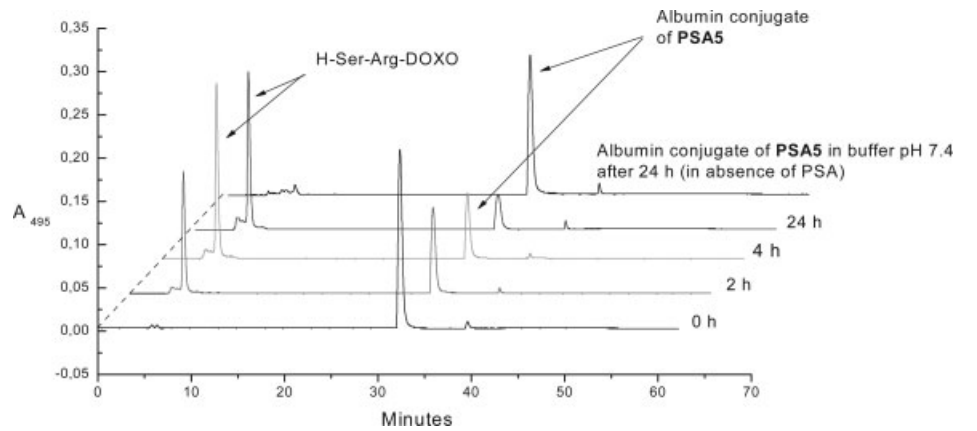

Figure 3 – Chromatograms of incubation studies with the albumin conjugate of **PSA5** in the presence of human PSA after 0, 2, 4 and 24 hr at 37°C. The concentration of the albumin conjugate of **PSA5** was 110 μM.

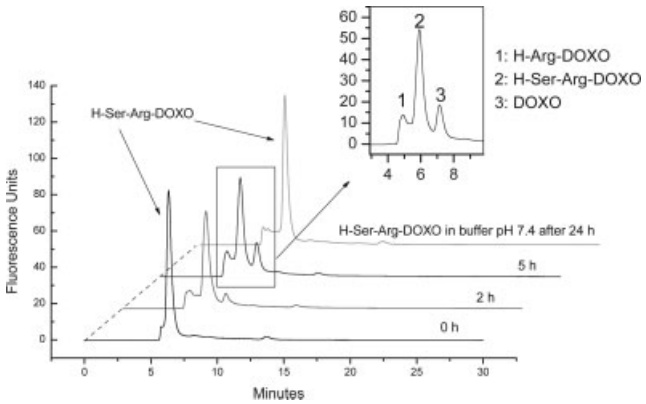

FIGURE 4 – Chromatograms of incubation studies of LNCaP tissue homogenate with H-Ser-Arg-DOXO after 0, 2 and 5 hr at 37°C. Concentration of H-Ser-Arg-DOXO was 125 μM.

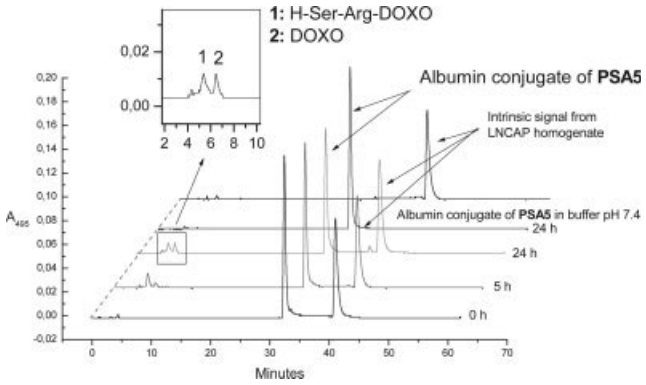

FIGURE 5 – Chromatograms of incubation studies of LNCaP tissue homogenate with the albumin conjugate of **PSA5** after 0, 5 and 24 hr at 37°C. Concentration of albumin conjugate of PSA5 was 100 μM.

riod of 3 weeks. The weight of the animals was checked 3 times weekly to monitor the well-being of the animals. After the second injection with free doxorubicin, animal weights in this group decreased drastically, and 2 animals from this group died (Fig. 7*b*); as a consequence the treatment had to be stopped. No toxicity was observed with **PSA5** and 3 × 12 mg/kg could be administered without a decrease in body weight.

Using bioluminescence measurements, the growth of the tumor was checked once weekly. Doxorubicin (until the treatment was stopped), and the prodrug at 12 mg/kg, markedly reduced the growth of the tumor (Fig. 7*c*). Termination of the doxorubicin treatment resulted in a resumption of tumor growth, and a restoration of the tumor signals to almost the level of the control tumors (Fig. 7*c*). In contrast, the bioluminescence signal for the **PSA5** treated animals remained at a relatively constant level over the period of the treatment indicating stable disease (Fig. 7*c*).

PSA5 and doxorubicin activity in an ortotopic prostate tumor model—Necropsy results

After 3 weeks of treatment (38 days after implantation) the animals were sacrificed, and tumor sizes were measured. Furthermore, organs that are potential targets for metastases from the LNCaP tumors (kidney, liver, spleen, intestine, the inguinal lymph nodes and lungs as well as a sample of the femur), were harvested, homogenized and assayed for luciferase activity as a measure for tumor cell infiltration of the organs. A part of the primary tumor was also homogenized and subjected to a luciferase assay.

The antitumor activity of **PSA-5** at 12 mg/kg noted by the *in vivo* measurement was confirmed with the callipered tumor sizes. Tumor sizes in this group were reduced by 62% (±25%, $^{**}p = 0.003$) compared to control tumors. Doxorubicin, on the other hand resulted in a reduction of the tumor burden by 33% (±37%, $p = 0.08$), which was not significant to controls (Fig 8*a*, left panel). The results from the *in vitro* luciferase assays generally correlated well with the tumor sizes [Figs. 8*a* (right panel) and 8*b*], and further confirmed the effect of the prodrug at 12 mg/kg [−50%, (SD ± 32)%, $^{**}p = 0.007$]. However, the tumor size reduction detected when callipering the tumors of doxorubicin treated animals, although smaller than for **PSA5**, was not con-

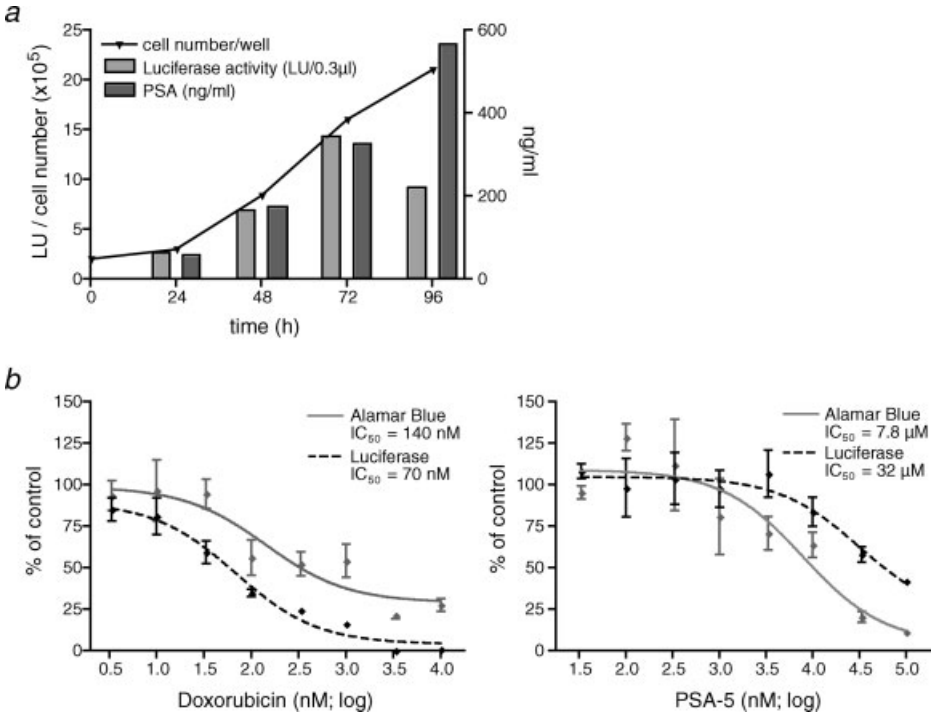

FIGURE 6 – (*a*) PSA secretion and luciferase activity of LNCaP cells *in vitro*. LNCaP LN cells were plated into the wells of a 6 well plate. 24, 48, 72 and 96 hr after, the medium was removed and PSA levels were determined. Cells were then trypsinized, counted, lysed in luciferase assay buffer and the luciferase activity was determined. Shown are the cell counts (line), luciferase activity (LU/0.3 μL of lysate; light grey bars) and PSA values (ng/mL, dark grey bars). (*b*) Determination of the IC_{50} of doxorubicin and **PSA5** on LNCaP LN cells *in vitro*. LNCaP LN cells were plated into a 96-well plate. 24 hr later, serial dilutions of the drugs were added in triplicates. Survival curves, plotted as percent of control, are shown from the Alamar Blue results (grey line) and the luciferase assay (black dotted line).

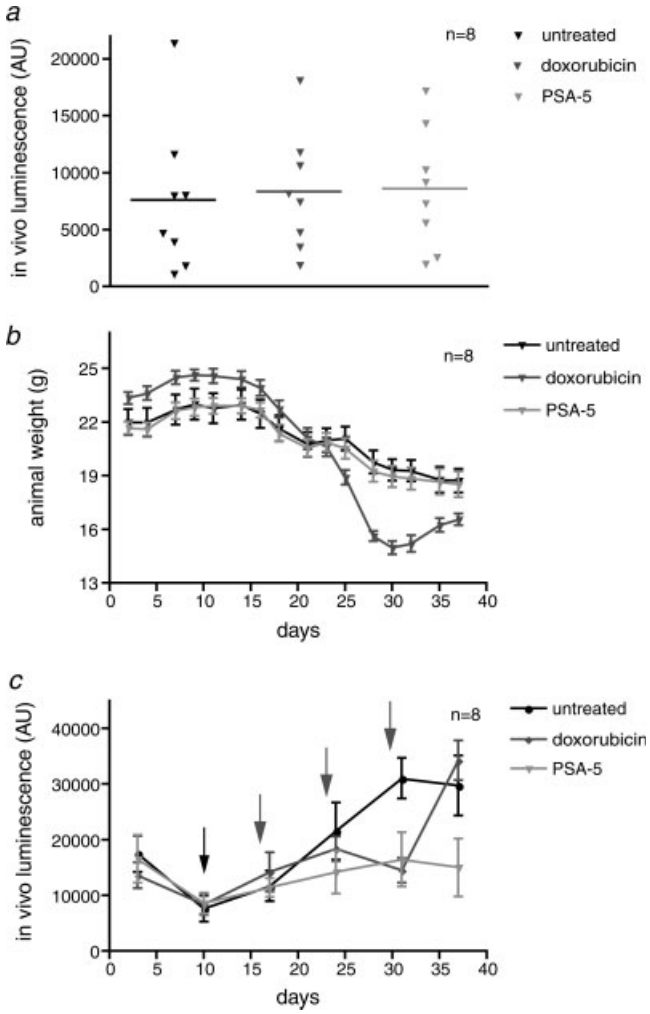

Figure 7 – (*a*) Randomization of animals according to luciferase signals from the primary tumor. Animals were injected with luciferin, and exposed to the Nightowl camera for 5 min. at 10 × 10 binning. Signals were quantified graphically, and the animals distributed according to the 4 treatment groups ($n = 8$). (*b*) Animal weights during treatment ($n = 8$). To monitor drug side effects, animals were weighed 3 times weekly. Two animals of the doxorubicin group died at days 28–30. (*c*) Tumor growth curve. *In vivo* bioluminescence was determined once weekly (as in *a*), and the results plotted graphically ($n = 8$). The black arrow indicates the time-point of the randomization, the grey arrows of the treatments. Note that, because of toxicity, doxorubicin could only be applied twice.

firmed in the luciferase assay (Fig 8*a*, right panel). In this respect, the *ex vivo* luciferase measurements correlated better with the *in vivo* signals, which also suggested similar tumor sizes between control and doxorubicin treated tumors. As in previous experiments, the luciferase assay mediated analysis of the metastatic spread of tumor cells to the organs of mice bearing LNCaP tumors suggested that the lung is the main target organ for metastases (Fig. 8*c*, left panel). When compared to lungs from control animals, those originating from mice treated with **PSA-5** displayed a significantly reduced luciferase activity [−50%, (SD ± 115)%, $*p = 0.038$; −95%, (SD ± 6)%, $**p = 0.0037$ if the deviation value is excluded], suggesting that the treatment either prevented the tumor cells from spreading to the lungs or from proliferating there (Fig. 8*c*, right panel). Doxorubicin treatment also reduced the spread of tumor cells to the lung, albeit not significantly [−76%, (SD ± 19)%, $p = 0.059$].

Luciferase activity and immunohistochemistry of lung and tumor sections

To ensure that the luciferase signals obtained from lung homogenates reflected metastases, sections were prepared from the frozen half of the lung of mice bearing LNCaP LN tumors and exposed to the CCD camera in the presence of luciferin and ATP. Distinct signals were obtained from the sections, which could be correlated with tumor cells in the lungs after performing H&E staining to reveal their morphology (Fig. 9*a*). When stained with a Cytokeratin-18 antibody, they scored positive, identifying them as of human epithelial origin (Fig. 9*b*).

Since a leaky vasculature is a prerequisite for the EPR-effect involved in the targeting of albumin-bound drugs to the tumor, a CD31 staining was prepared from a LNCaP LN tumor. As already suggested by the dark red, hemorrhagic appearance of the tumors, the vasculature revealed by the CD31 antibody is extremely dense with no apparent organization (Fig. 9*c*).

Discussion

Albumin-binding prodrugs have the potential of reducing the side effects and improving the efficacy of anticancer agents. Anthracyclines have frequently been used for the development of such prodrugs.[19] An acid-sensitive doxorubicin prodrug, *i.e.*, the (6-maleimidocaproyl)hydrazone derivative of doxorubicin (DOXO-EMCH) showed good tolerability and antitumor efficacy in a recently completed phase I study and will enter phase II studies in 2007.[20] Uptake of albumin is mediated by the EPR effect, *i.e.*, enhanced permeability and retention of macromolecules in relation to passive tumor targeting.[21] The entry of macromolecules into tumors is mediated by a "leaky" vascular network of viable tumor tissue in contrast to the blood vessels in most normal tissues, which have an intact endothelial layer allowing the diffusion of small molecules but not the entry of macromolecules into the tissue. Since tumor tissue does not generally have a lymphatic drainage system, macromolecules are retained and can accumulate in solid tumors.

In general, a high degree of protein-binding, especially to albumin, is considered a disadvantage because only the free drug can exert its pharmacological effect. *In situ* binding of prodrugs to albumin turns this potential disadvantage into a therapeutic benefit by incorporating a cleavable bond between the drug and the albumin-binding moiety that ensures a specific release of the drug at its site of action. As a consequence, the therapeutic index of DOXO-EMCH is significantly enhanced allowing high doses to be administered to tumor-bearing animals with a concomitant increase in antitumor activity compared to free doxorubicin.[19]

In this work, we developed an albumin-binding doxorubicin prodrug EMC-Arg-Ser-Ser-Tyr-Tyr—Ser-Arg-DOXO (**PSA5**) that is cleaved by PSA releasing the doxorubicin dipeptide H-Ser-Arg-DOXO. Incubation studies with LNCaP tumor homogenates demonstrated that this dipeptide is cleaved to H-Arg-DOXO and doxorubicin, presumably by further proteases. This cleavage pattern can be judged as an improvement over our first PSA cleavable doxorubicin prodrug EMC-Arg-Arg-Ser-Ser-Tyr-Tyr—Ser-Gly-DOXO, which yielded the doxorubicin dipeptide H-Ser-Gly-DOXO after PSA cleavage which was not, however, further degraded in tumor homogenates.[9]

In confirmation of our earlier results with PSA cleavable doxorubicin prodrugs,[9] **PSA5** showed significantly higher IC_{50} values than doxorubicin in the PSA-positive cell line LNCaP presumably due to low PSA levels secreted in the cell culture medium. In contrast, in subsequent *in vivo* experiments **PSA5** showed superior antitumor efficacy at 3 × 12 mg/kg doxorubicin equivalents over doxorubicin at a dose of 2 × 4 mg/kg. It should be noted that **PSA5** at this dose schedule showed no noteworthy decrease in body weight in contrast to doxorubicin treated animals that showed a significant decrease in body weight (see Fig 7*b*) as well as toxic deaths indicating clearly that the dose of 2 × 4 mg/kg doxorubicin cannot be exceeded.

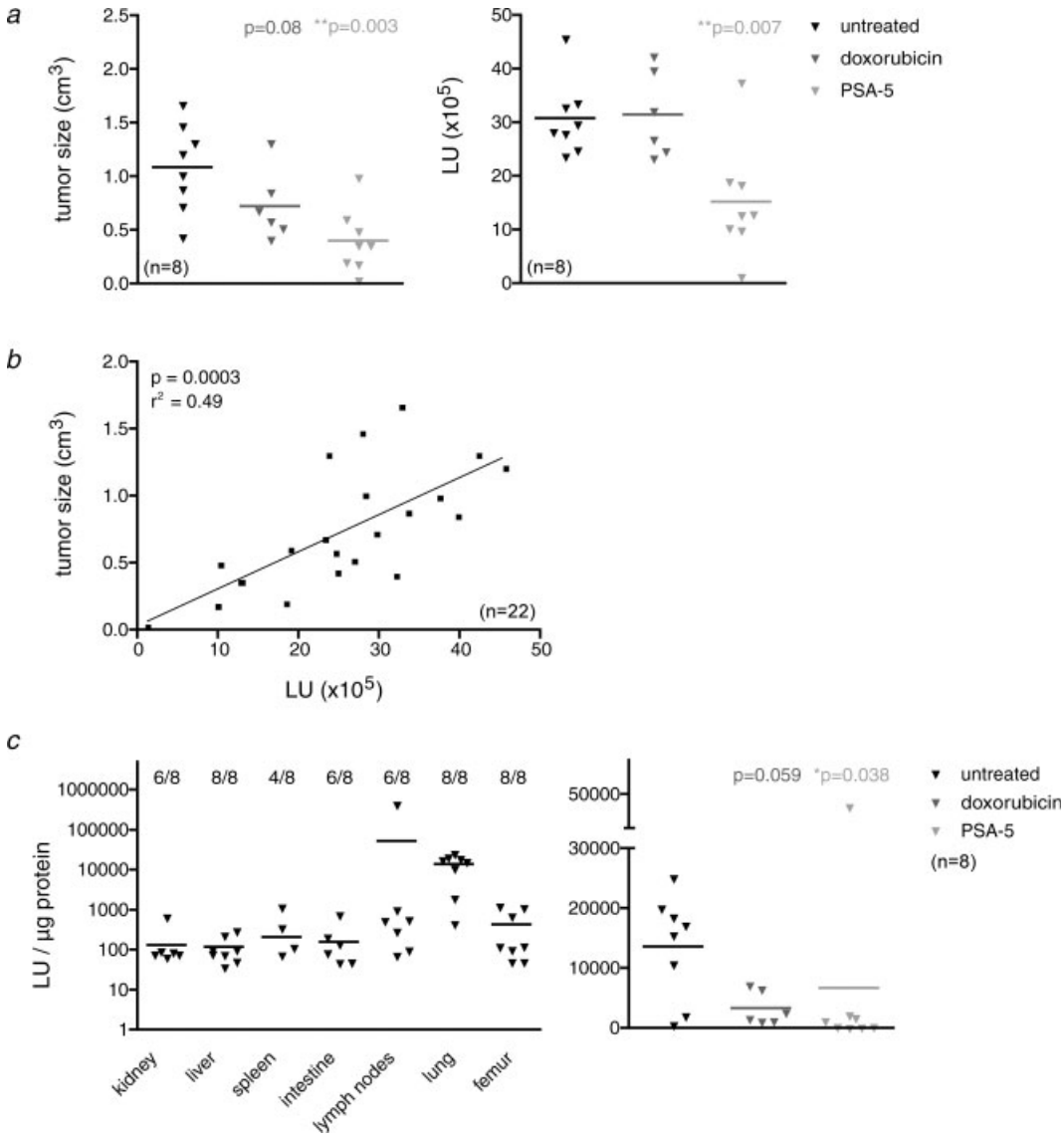

FIGURE 8 – (*a*) Scatter graphs for tumor volumes (left) and luciferase activity (right) ($n = 8$; doxorubicin: $n = 6$). Tumors were resected from the animals, and the size determined using a caliper. One half was then homogenized, and the luciferase activity assayed from the lysate as described in materials and methods. *p* values were determined using the Mann–Whitney test. (*b*) Linear regression analysis of tumor size *versus* luciferase activity ($n = 22$). The earlier results were plotted against each other, and the correlation and *p* values determined. (*c*) Luciferase assays from mouse organs. Organs were homogenized, and the luciferase activity assayed from the lysates as described in "Materials and methods" section. The results are shown as scatter graphs, left all organs tested from control animals, right from the lungs of all animals, displayed according to the treatment groups ($n = 8$). *p* values were determined using Mann–Whitney test.

Therapy with **PSA5**, however, was well-tolerated and showed significant antitumor activity on the primary tumor as well as on the number of metastases up to the end of the experiment. The *in vivo* result thus demonstrates that the therapeutic index of doxorubicin is improved with **PSA5**. The main reason for this improvement is presumably a more favorable biodistribution concomitant with a relative tumor accumulation of doxorubicin in the primary tumor and metastases. Results with an anti-CD31-antibody indicate a high degree of vascular disorder; together with their dark red appearance, orthotopically implanted LNCaP tumors seem to be highly vascularized and suitable for passive targeting with albumin.

The use of a luciferase marked LNCaP prostate cell line in our study allowed the randomization of the animals at the beginning of drug treatment as well as the exclusion of non-tumor bearing animals. Since the take-rate in this model is only 60–70%, the latter issue is of crucial importance. Moreover, drug effects could be monitored *in vivo*, despite the orthotopic implantation of the tumors. Up to the time point when the treatment had to be stopped because of toxicity, the efficacy of the free doxorubicin could be shown to be relatively similar to that of the **PSA5** prodrug. At the time of necropsy the *in vivo* bioluminescence signal suggested a resumption of tumor growth in the doxorubicin group to almost the levels of the controls. Although analysis of the tumor sizes revealed a slight reduction of primary tumor size when compared to the controls, this was not significant. *In vitro* luciferase assays, however, confirmed the *in vivo* bioluminescence analysis, suggesting a lack of efficacy of the doxorubicin treatment on the primary tumor. The slight discrepancy between tumor size measurements and luciferase *in vivo*/*in vitro* assays might be explained by a faster recovery of tumor cells from the treatment than the surrounding stromal cells, resulting in smaller tumors with higher lu-

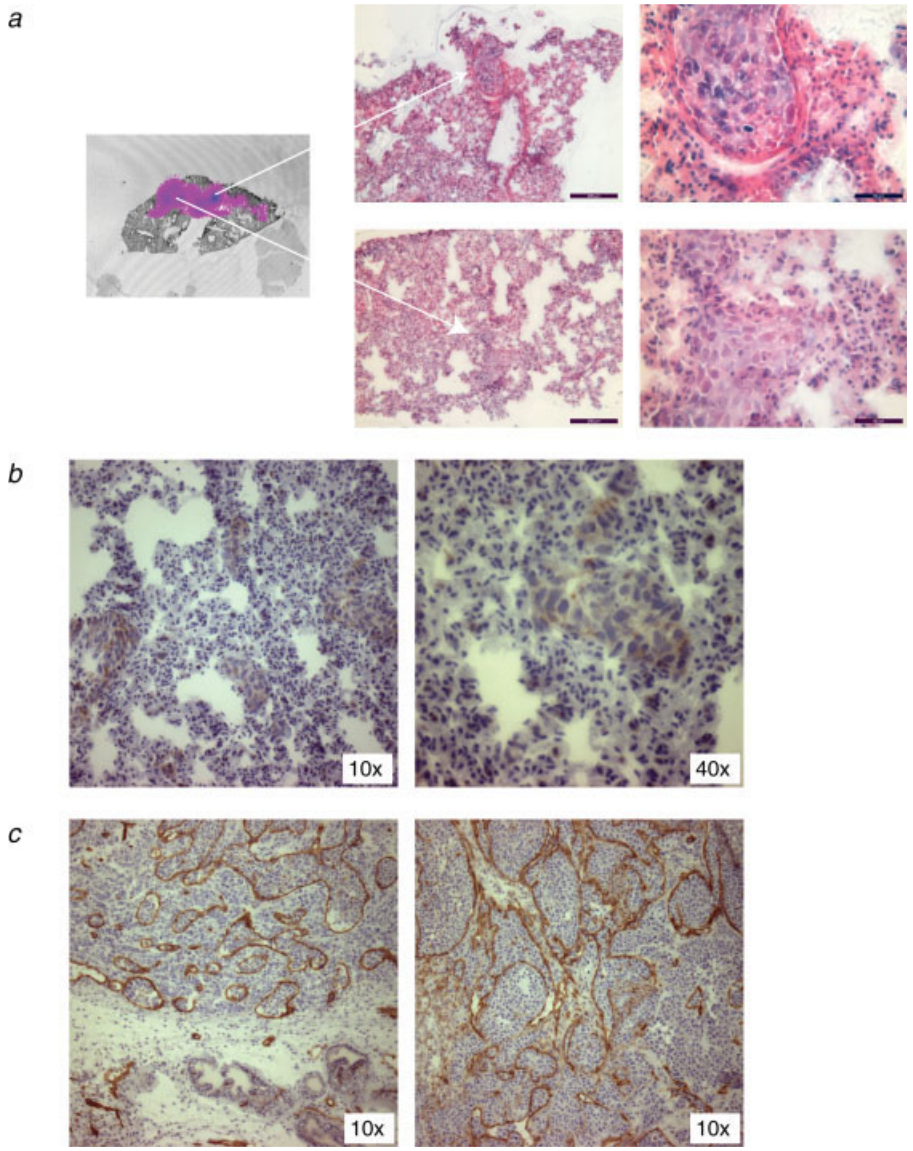

FIGURE 9 – (*a*) Luciferase activity measurement and subsequent H&E-staining of a lung section. A cryosection was prepared from lung tissue, incubated with luciferin and ATP and exposed to a CCD camera for 2 min. at 1 × 1 binning. The section was then washed and stained with H&E. On the left, the overlay is shown of the H&E stain with the luciferase signal. To the right, 10× and 40× magnifications of the positive scoring areas are shown. In the luciferase assay, the other half of this lung produced 25,000 LU/μg protein. (*b*) Cytokeratin 1–8 staining of lung tissue. A cryo-section of a lung was stained using a CK1–8 antibody, and counter-stained using hematoxylin. Positively scoring human tumor cells are labeled brown. A 10× and a 40× magnification are shown. (*c*) CD31 staining of LNCaP LN tumor tissue. A section of a tumor was stained using a CD31 antibody, and counter-stained using hematoxylin. Note the large, positively brown stained endothelial vessel-like structures in the tumor tissue. [Color figure can be viewed in the online issue, which is available at www.interscience.wiley.com.]

ciferase activity. Besides measuring apparent tumor size *in vivo* and tumor cell content of the primary tumor *in vitro*, luciferase assays may also be used to measure tumor cell spreading into organs as a measure for metastatic disease. Both the free drug and the prodrug decreased the metastatic spread of LNCaP LN cells to the lung, albeit in the case of doxorubicin this effect was just below statistical significance. The more marked effect of doxorubicin on lung metastases than on the primary tumor suggests that during the treatment period the level of tumor cells infiltrating the lungs was reduced and once treatment was stopped, the resumption of the metastatic process was not as efficient as that of the primary tumor growth.

Besides albumin-binding prodrugs of doxorubicin that aim to exploit PSA as a molecular target, 2 low-molecular weight doxorubicin prodrugs have been developed that are cleaved by PSA.[22–24] These doxorubicin derivatives include the peptide sequences Mu-His-Ser-Ser-Lys-Leu-Gln-Leu-OH (Mu = morpholinocarbonyl) and *N*-glutaryl-(hydroxypropyl)-Ala-Ser-cyclohexylglycyl-Gln-Ser-Leu-OH (abbreviated L-377,202) bound to the amino position of doxorubicin. Both low-molecular weight prodrugs were designed to release *N*-(L-leucyl)doxorubicin after cleavage by PSA.

The MTD of both prodrugs was ~5–7-fold higher than for free doxorubicin, and at these doses they demonstrated significant antitumor activity in PSA-positive animal models (LNCaP, CWR22, PC 82).[23,24] A phase I study has been carried out with L-377,202 with 225 mg/m^2 being established as the MTD in this study that corresponds to ~90 mg/m^2 doxorubicin equivalents.

In summary, we have developed a novel albumin-binding prodrug of doxorubicin that is cleaved by PSA releasing doxorubicin as the final cleavage product and shows promising antitumor efficacy in an orthotopic prostate tumor model.

Experimental section

Chemicals, Materials and Spectroscopy

Chemicals and solvents were purchased from Sigma-Aldrich, Fluka, Merck, KMF, LGC Promochem and Roth and were used without further purification. Doxorubicin hydrochloride was purchased from Yick-Vic Chemicals & Pharmaceuticals (HK) China. EMC-Arg-Ser-Ser-Tyr-Tyr-Ser-Arg-OH was custom-made by JPT Peptide Technologies GmbH, Berlin, Germany. Human serum albumin (5% solution) was purchased from Octapharma GmbH, Langenfeld, Germany that contained ~60% free thiol groups as assessed with the Ellmann's test. The buffers used were vacuum-filtered through a 0.2 μm membrane (Sartorius AG, Göttingen, Germany) and thoroughly degassed with ultrasound prior to use.

Enzymatically active PSA was purchased from Calbiochem (Bad Soden, Germany). Xenograft tumor tissues were gratefully received from Dr. I. Fichtner (EPO Exp. Pharmakol. & Onkol. GmbH, Berlin). Lyophilization was performed with a lyophilizer Alpha 2–4 (Christ, Osterode, Germany).

UV/vis-spectrophotometry was carried out with a double-beam spectrophotometer U-2000 from Hitachi. Mass spectra (ESI-MS) was performed with a Thermoelektron LCQ Advantage.

Chromatography

Column chromatographic separations were carried out as flash chromatography using reverse-phase Lichroprep® RP-C18 from Merck with a particle size of 0.040–0.063 mm. HPLC for the determination of purity of **PSA5** was performed with a Waters System (pump: Waters 616, detector: Waters 996 Photodiode Array Detector; controller: Waters 600S; auto sampler: Waters 717; Empower PDA software); column: Waters Symmetry® C18 (300–5, 250 × 4.6 mm^2) with pre-column; chromatographic conditions: flow: 1.2–1.8 mL/min; mobile phase A: 70% MeCN, 30% 20 mM potassium phosphate (pH 7.0), mobile phase B: 27.5% MeCN, 72.5% 20 mM potassium phosphate (pH 7.0), gradient: 0–26 min 100% mobile phase B; 26–41 min increase to 100% mobile phase A; 41–50 min 100% mobile phase A; 50–60 min decrease to 100% mobile phase B; injection volume: 50 μL.

HPLC for incubation and stability studies with **PSA5** and the respective albumin-conjugate was performed with BioLogic Duo Flow System from Bio-Rad (Munich, Germany), which was connected with a Merck F-1050 Fluorescence Spectrophotometer (EX. 490 nm, EM. 540 nm) or a Lambda 1,000 visible detector from Bischoff (at λ = 495 nm); UV-detection at 280 nm; column: Waters, 300 Å, Symmetry C18 (4.6 × 250 mm^2) with precolumn; chromatographic conditions: flow: 1.2 mL/min; mobile phase A: 27% MeCN, 73% 4 mM sodium phosphate buffer (pH 3.0); mobile phase B: 70% MeCN, 30% 4 mM sodium phosphate buffer (pH 3.0); gradient: 0–25 min 100% mobile phase A; 25–40 min increase to mobile phase B; 40–50 min 100% mobile phase B; 50–60 min decrease to initial mobile phase; injection volume: 50 μL.

Synthesis of H-Arg-DOXO. Doxorubicin hydrochloride (200 mg, 0.35 mmol), Fmoc-Arg-OH (305 mg, 0.77 mmol) and triethylamine (191 μL, 139.4 mg, 1.38 mmol) were dissolved in 25 mL of anhydrous DMF. After stirring at room temperature for 5 min, HATU (157 mg, 0.41 mmol) was added. After stirring at room temperature for 2 hr, the product was precipitated with 1,000 mL of diethyl ether, washed 3 times with diethyl ether and dried in vacuum to yield 400 mg of a red powder.

The protecting group was removed by dissolving 400 mg Fmoc-Arg-DOXO in 5 mL of 20% piperidine solution (DMF) and stirring for 5 min. The violet product was precipitated with 250 mL of diethyl ether, washed 3 times with diethyl ether and dried in vacuum. The product was purified on a diol column using chloroform/methanol 3:1 + 0.1% TFA. The remaining product on the column was eluted with chloroform/methanol 2:1 + 0.1% TFA to afford 323 mg of H-Arg-DOXO as a red powder after precipitating the combined fractions containing the product with diethyl ether. Mass [ESI-MS: 2.5 kV]: m/z = 700.2 $[M + H]^+$, 722.2 $[M + Na]^+$; HPLC (495 nm): >95%.

Synthesis of H-Ser-Arg-DOXO. H-Arg-DOXO (390 mg, 0.558 mmol), Fmoc-Ser-OH (391 mg, 1.192 mmol) and DIEA (50 mg, 426 μL, 2.512 mmol) were dissolved in 22 mL of anhydrous DMF. After stirring at room temperature for 5 min, HATU (318 mg, 0.837 mmol) was added. After stirring at room temperature for 2 hr, the product was precipitated with 200 mL of diethyl ether, washed 3 times with diethylether and dried in vacuum.

The product was purified on a diol column using chloroform/methanol 5:1 + 0.1% TFA to afford 410 mg Fmoc-Ser-Arg-DOXO as a red powder after precipitating the combined fractions containing the product with diethyl ether.

The protecting group was removed by dissolving 400 mg Fmoc-Ser-Arg-DOXO in 8 mL of 20% piperidine solution (DMF) and stirring for 5 min. The product was precipitated with 400 mL of diethyl ether, washed 3 times with ether and dried in vacuum to afford 312 mg of H-Ser-Arg-DOXO. Mass (ESI-MS: 3 kV): m/z 788.2 $[M+H]^+$; HPLC (495 nm): >95%.

Synthesis of EMC-Arg-Ser-Ser-Tyr-Tyr-Ser-Arg-DOXO (2TFA) (PSA5). H-Ser-Arg-DOXO (128 mg, 0.163 mmol), EMC-Arg-Ser-Ser-Tyr-Tyr-OH (159.3 mg, 0.184 mmol), HOBt (65.9 mg, 0.487 mmol) and 4-methylmorpholine (71 μL, 65 mg, 0.643 mmol) were dissolved in 10 mL of anhydrous DMF; after stirring at +5°C for 15 min, DIPC (151 μL, 123 mg, 0.975 mmol) was added. After stirring at +5°C for 72 hr, the product was precipitated with diethyl ether, washed 3 times with diethylether and dried in high vacuum. The product was dissolved in methanol/water 3:1 and purified first through size-exclusion chromatography on Sephadex™ LH-20 (Amersham Pharmacia Biotech AB) using methanol and in a second purification step on a reverse-phase column using acetonitrile/water + 0.1% TFA 30:70 to afford 152 mg of **PSA5** as a red powder after lyophilizing the combined fractions containing the product. Mass (LC-MS-pos. ESI. 1.5 kV): m/z 1,636.5 $[M]^+$, 1,749.7 $[M^+ + CF_3COO^-]$, 1,750.7 $[M^+ + CF_3COOH]$; HPLC (495 nm): >98%.

Synthesis of the albumin conjugate of PSA5. 1.9 mg of **PSA5** were dissolved in 2 mL human serum albumin (5% solution from Octapharma) and the solution was incubated at 37°C for 1 hr. The albumin conjugate was obtained after subsequent size-exclusion chromatography (Sephacryl® S-100; Tris-buffer: 50 mM Tris-HCl - pH 7.4). The content of anthracycline in the sample was determined using the ε-value for doxorubicin [ε_{495} (pH 7.4) = 10,650 M^{-1} cm^1]. The concentration of **PSA5** in the conjugate was adjusted to 400 ± 50 μM by concentrating the sample with CENTRIPREP®-10-concentrators from Amicon, FRG (4°C and 4,500 rpm). Samples were kept frozen at −20°C and thawed prior to use.

Incubation studies with human blood plasma. Human blood plasma (EDTA stabilized) was taken from healthy volunteers. 1.8 mg of **PSA5** were dissolved in 200 μL of 10 mM sodium phosphate/5% D-glucose buffer pH 6.4 to give a 5 mM stock solution of **PSA5**. 30 μL was added to plasma preincubated at 37°C at a final concentration of 250 μM and the samples were incubated for 5 min, 4, 20 hr and for 24 hr at 37°C. A 50 μL sample for each time point was analyzed by HPLC.

In a further experiment 500 μL of human blood plasma was preincubated with 0.4 mg of EMC for 1 hr. Subsequently, 10 μL of **PSA5** and 190 μL of the preincubated plasma was mixed and incubated for 10 min. 50 μL samples were analyzed with HPLC.

Incubation studies of the albumin conjugate of PSA5 with PSA at pH 7.4. 100 μL of the albumin conjugate stock solution (420 μM) of **PSA5** were mixed with 50 μL PSA (200 μg/mL) and 50 μL of buffer (Tris-buffer pH 7.4). The samples were incubated at 37°C. After 5 min, 1.5, 3 and 24 hr samples were collected and 50 μL of each sample were diluted 1:1 to a final concentration of 110 μM and analyzed by HPLC.

Preparation of LNCaP tumor tissue homogenates at pH 7.4. For obtaining LNCaP carcinoma tissue homogenates, all steps were carried out on ice where possible. Tissue of LNCaP xenograft tumors were cut into small pieces, and 200 mg samples were transferred in a 2 mL Eppendorf tube to which was added 800 μL of homogenate buffer (50 mM Tris-HCl buffer, pH 7.4 containing 1 mM monothioglycerol). Homogenization was carried out with a micro-dissmemberator at 3,000 rpm for 3 min with the aid of glass balls, and the samples were then centrifuged at 5,000 rpm for 10 min and kept frozen at −78°C prior to use.

Incubation studies of the albumin conjugate of PSA5 with LNCaP tissue homogenates. The albumin conjugate of **PSA5** was incubated with LNCaP tissue homogenate at 37°C at a final concentration of 100 μM and chromatograms recorded at 495 nm using reverse phase HPLC at the time points stated in the figures.

In vitro cellular experiments. For the PSA/luciferase measurement, cells were plated at 200,000 cells/well into a 6-well plate. After 24, 48, 72 and 96 hr, medium supernatant was removed and stored at −80°C. Cells were then trypsinized, counted and cells frozen as a cell pellet. Once all samples were collected, the cell pellets were lysed in 90 μL of luciferase assay buffer (25 mM TRIS-phosphate pH 7.8; 2 mM EDTA; 2 mM DTT; 0.1% Triton X-100), and 10 μL of the undiluted, as well as 1/10 and 1/100 dilutions were measured in a Luminometer (BMG Lumistar) using the luciferase substrate from Promega (Promega E4550), according to the manufacturer's instructions. PSA values were determined nephometrically with a microparticale immunoassay from Abbot.

For IC_{50} measurements, 0.2×10^4 cells were plated per well in a 96-well plate. 24 hr later, serial dilutions of the drugs were added in triplicates. alamar blue was added to the medium after 69 hr, and the cells were incubated for another 3 hr, before the fluorescence was measured at 590 nm. Cells were then lysed in 100 μL of luciferase assay buffer, and an aliquot of the lysate was assayed for luciferase activity.

Animal experiments. All animal experiments were performed in accordance to German Animal License Regulations (Tierschutzgesetz) identical to UKCCCR Guidelines for the welfare of animals in experimental neoplasia.[18] Male SCID (C.B-17/Icr-HanHsd-Prkdc-scid) mice were obtained from Harlan Winkelmann GmbH, Germany.

Mice were anesthetized with isofluorane, positioned and fixed on the back. The coat of the abdominal area was shaved and the skin was disinfected with alcohol (70%). A 3–4-mm incision was made alongside the linea alba in the lower abdomen using the cranial edge of the bladder for orientation. Seminal vesicles and prostate were pulled out partially and exposed carefully. 2×10^6 tumor cells, suspended in 20 μL PBS, were injected into the anterior part of the prostate using a 29-gauge needle syringe. The exteriorized organs were reinserted into the abdomen, the abdominal wall was closed using 5-0 Dexon sutures (DEXON®, B.Braun-Dexon, Spangenberg, Germany), and the skin was again disinfected using a Dibromol tincture (Trommsdorf GmbH, Germany).

Measurement of in vivo bioluminescence. The animals were injected with 100 μL of D-luciferin (Synchem OHG, Germany), and anesthesized using isofluorane. 10 min. after the injection, the mice were transferred into a NIGHTOWL camera (Berthold Technologies) equipped with isofluorane adaptors. An overview picture of the mice as well as 2 exposures, 5 min at 10×10 binning and 1 min at 2×2 binning were taken.

Raw, unmodified images from the camera were imported into Adobe Photoshop 7.0® and transformed to 8-bit indexed color format. To help visualizing the primary tumor, levels were set to 0-25, and the color table "spectrum" was applied (the latter 2 steps did not change the information content of the files, only helped to localize the signal for the graphical quantification in ImageJ). The files were then opened in imageJ, and the mean pixel intensity of 150-pixel squares drawn at the site of the primary tumor was measured; the results were used to generate growth curves.

Necropsy and luciferase assays of mouse organs. Mice were sacrificed, the abdominal cavity was opened and a picture of the tumor *in situ* was taken. The primary tumor was resected, measured and its volume was calculated using the formula $V = a^2 \times A/2$ (a - small diameter, A - large diameter). Tumors were weighed and cut in 2 pieces. One was shock frozen in liquid nitrogen for histology, the other homogenized in 2 mL of luciferase lysis buffer. To obtain a quantitative analyze of the metastatic spread into potential target organs, the kidney, liver, spleen and lungs as well as a sample of the femur, were resected from the animals taking great care to prevent cross-contamination of the tissues. Whereas a part of these organs were also cryo-preserved, samples from the intestine and the inguinal lymph nodes were only analyzed in luciferase assays. After homogenization, insoluble material was spun 10 min at 3,000 rpm in a Heraeus Megafuge 2.0. 5 μL were checked for protein concentration using a Bradford assay (Sigma B6916) with BSA serving as a standard protein, and 10 μL were measured in a luciferase assay (Promega E4550).

Histology. 7 μm cryo-sections were prepared, and either processed for immunohistochemistry or assayed for luciferase activity, followed by H&E staining. For the former, the sections were fixed using 4% paraformaldehyde and stained for human cytokeratin using the biotinylated mouse monoclonal pan cytokeratin 1–8 antibody from Progen (Cat # 61506) according to the instructions from the manufacturer. In the latter case, the sections were overlaid with a luciferase substrate mix (Promega E4550), exposed under a Nightowl camera (Berthold) for 2 min. at 1×1 binning, washed in water and stained with H&E to reveal the morphology of the sections.

Acknowledgements

The support of the Dietmar Hopp Foundation is gratefully acknowledged.

References

1. Arlen PM, Gulley JL. Docetaxel-based regimens, the standard of care for metastatic androgen-insensitive prostate cancer. Future Oncol 2005;1:19–22.
2. Lilja H, Abrahamsson PA, Lundwall A. Semenogelin, the predominant protein in human semen. Primary structure and identification of closely related proteins in the male accessory sex glands and on the spermatozoa. J Biol Chem 1989;264:1894–900.
3. Akiyama K, Nakamura T, Iwanaga S, Hara M. The chymotrypsin-like activity of human prostate-specific antigen, gamma-seminoprotein. FEBS Lett 1987;225:168–72.
4. Yu H, Diamandis EP, Levesque M, Sismondi P, Zola P, Katsaros D. Ectopic production of prostate specific antigen by a breast tumor metastatic to the ovary. J Clin Lab Anal 1994;8:251–3.
5. Diamandis EP, Yu H, Sutherland DJ. Detection of prostate-specific antigen immunoreactivity in breast tumors. Breast Cancer Res Treat 1994;32:301–10.
6. Yu H, Diamandis EP, Sutherland DJ. Immunoreactive prostate-specific antigen levels in female and male breast tumors and its association with steroid hormone receptors and patient age. Clin Biochem 1994;27:75–9.
7. Levesque M, Hu H, D'Costa M, Diamandis EP. Prostate-specific antigen expression by various tumors. J Clin Lab Anal 1995;9:123–8.
8. Diamandis EP. New diagnostic applications and physiological functions of prostate specific antigen. Scand J Clin Lab Invest Suppl 1995; 221:105–12.
9. Kratz F, Mansour A, Soltau J, Warnecke A, Fichtner I, Unger C, Drevs J. Development of albumin-binding doxorubicin prodrugs that are cleaved by prostate-specific antigen. Arch Pharm (Weinheim) 2005;338: 462–72.
10. Kratz F, Mueller-Driver R, Hofmann I, Drevs J, Unger C. A novel macromolecular prodrug concept exploiting endogenous serum albumin as a drug carrier for cancer chemotherapy. J Med Chem 2000; 43:1253–6.
11. Kratz F, Warnecke A, Scheuermann K, Stockmar C, Schwab J, Lazar P, Drückes P, Esser N, Drevs J, Rognan D, Bissantz C, Hinderling C, et al. Probing the cysteine-34 position of endogenous serum albumin with thiol-binding doxorubicin derivatives: improved efficacy of an acid-sensitive doxorubicin derivative with specific albumin-binding properties compared to that of the parent compound. J Med Chem 2002;45:5523–33.
12. Mansour AM, Drevs J, Esser N, Hamada FM, Badary OA, Unger C, Fichtner I, Kratz F. A new approach for the treatment of malignant melanoma: enhanced antitumor efficacy of an albumin-binding doxorubicin prodrug that is cleaved by matrix metalloproteinase 2. Cancer Res 2003;63:4062–6.
13. Chung DE, Kratz F. Development of a novel albumin-binding prodrug that is cleaved by urokinase-type-plasminogen activator (uPA). Bioorg Med Chem Lett 2006;16:5157–63.
14. El Hilali N, Rubio N, Blanco J. Different effect of paclitaxel on primary tumor mass, tumor cell contents, and metastases for four experimental human prostate tumors expressing luciferase. Clin Cancer Res 2005;11:1253–8.
15. Bornmann C, Graeser R, Esser N, Ziroli V, Jantscheff P, Keck T, Unger C, Hopt UT, Adam U, Schaechtele C, Massing U, von Dob-

schuetz E. A new liposomal formulation of Gemcitabine is active in an orthotopic mouse model of pancreatic cancer accessible to bioluminescence imaging. Cancer Chemother. Pharmacol., 2007, in press (epub available).
16. Sato N, Gleave ME, Bruchovsky N, Rennie PS, Beraldi E, Sullivan LD. A metastatic and androgen-sensitive human prostate cancer model using intraprostatic inoculation of LNCaP cells in SCID mice. Cancer Res 1997;57:1584–9.
17. Stephenson RA, Dinney CP, Gohji K, Ordonez NG, Killion JJ, Fidler IJ. Metastatic model for human prostate cancer using orthotopic implantation in nude mice. J Natl Cancer Inst 1992;84:951–7.
18. Workman P, Balmain A, Hickman JA, McNally NJ, Rohas AM, Mitchison NA, Pierrepoint CG, Raymond R, Rowlatt C, Stephens TC, et al. UKCCCR guidelines for the welfare of animals in experimental neoplasia. Lab Anim 1988;22:195–201.
19. Kratz F, Warnecke A, Schmid B, Chung DE, Gitzel M. Prodrugs of anthracyclines in cancer chemotherapy. Curr Med Chem 2006,13, 477–523.
20. Kratz F. DOXO-EMCH (INNO-206), the first albumin-binding prodrug of doxorubicin to enter clinical trials. Expert Opin Investig Drugs 2007;16:855-866.
21. Maeda H, Wu J, Sawa T, Matsumura Y, Hori K. Tumor vascular permeability and the EPR effect in macromolecular therapeutics: a review. J Controlled Release 2000;65:271–84.
22. Denmeade SR, Nagy A, Gao J, Lilja H, Schally AV, Isaacs JT. Enzymatic activation of a doxorubicin-peptide prodrug by prostate-specific antigen. Cancer Res 1998;58:2537–40.
23. Khan SR, Denmeade SR. In vivo activity of a PSA-activated doxorubicin prodrug against PSA-producing human prostate cancer xenografts. Prostate 2000;45:80–3.
24. DeFeo-Jones D, Garsky VM, Wong BK, Feng DM, Bolyar T, Haskell K, Kiefer DM, Leander K, McAvoy E, Lumma P, Wai J, Senderak ET, et al. A peptide-doxorubicin 'prodrug' activated by prostate-specific antigen selectively kills prostate tumor cells positive for prostate-specific antigen in vivo. Nat Med 2000;6:1248–52.